THE PUBLISHING HOUSE
OF THE ROMANIAN ACADEMY

PROCEEDINGS OF THE ROMANIAN ACADEMY, Series A,
Volume 23, Number 1/2022, pp. 57–68

ANALYTICAL DESIGN AND APPLICATIONS OF 2D ANISOTROPIC FILTERS WITH ELLIPTICAL FREQUENCY RESPONSE

Radu MATEI

"Gheorghe Asachi" Technical University, Faculty of Electronics, Telecommunications and Information Technology
Institute of Computer Science, Romanian Academy – Iaşi Branch
Iaşi, Romania
E-mail: rmatei@etti.tuiasi.ro

Abstract. This paper describes an analytical design technique in the frequency domain for a particular class of two-dimensional zero-phase anisotropic filters, namely with an elliptical or circular frequency response. These filters may be low-pass, if their response contains the origin of the frequency plane, or band-pass. The elliptical filters are specified by their orientation angle and the lengths of its axes. Their synthesis begins from a Gaussian low-pass prototype with a given selectivity, its frequency response being a ratio of two factored, even order polynomials. A specific frequency transformation is next determined, which is applied to the 1D prototype, leading to the desired 2D elliptically-shaped filter. The frequency response of the obtained filter results in a factored, matrix form and it explicitly contains the imposed specifications. Thus the filter is parametric, it can be adjusted or tuned for various specifications, without the need to resume every time from the start the design procedure. The filters designed through this analytical method are accurate in shape and efficient, of relatively low order, and their frequency response results in a factored form, convenient for implementation. Some relevant examples of design using the proposed method and also some filtering tasks on various test images are provided, to show their capabilities in image processing applications.

Key words: 2D filters, approximations, analytical design, anisotropic, elliptical and circular filters.

1. INTRODUCTION

Two-dimensional filters have constantly developed as an essential research field, due to their important applications in digital image processing, and various design techniques emerged [1]. As an alternative to the well-known optimization methods based on numerical algorithms, generally leading to optimal filters for imposed specifications, there have been elaborated also analytical design methods with major advantages, such as a closed form of the filter frequency response and the tunability, or the possibility to adjust filter characteristics through their parameters. These analytic techniques rely on 1D prototypes, to which specific frequency transformations are applied, depending on the desired 2D filter. A convenient and largely used tool for 2D filter design is also the McClellan transform [2, 3]. There exist a large variety of 2D filters with various shapes, both of FIR and IIR type which find specific applications in image processing. A particular class are elliptically-shaped filters, approached in earlier and more recent papers such as [4–9]. They found useful applications in iris recognition [8], fingerprint enhancement [9] etc. Some elliptical filters have also Gaussian [5] or Gabor [9] characteristics. Filters with circular frequency response have also been developed [10, 11] and are also widely used. Efficient design of anisotropic Gaussian filters is achieved in [12, 13]. The author has also approached analytical design of some types of 2D elliptically-shaped filters in previous works [14–16]. Separable Gaussian directional FIR filters were approached in [17], while directional and square filters are described in [18]. Another class of zero-phase directional filters designed analytically is approached in [19]. Anisotropic filters are very useful due to their directional response.

This work proposes an analytical design method for parametric elliptical or circular 2D filters, with a Gaussian shape. The resulted filters are adjustable through specified parameters, controlling the selectivity and the peak frequency for band-pass filters. The design process starts from a 1D Gaussian prototype filter

with factored transfer function, to which a specific frequency mapping is applied, yielding the desired 2D filter frequency response, either elliptical or circular, which results directly factored, this being an important advantage in implementation. Several design examples as well as image filtering applications are provided.

2. GAUSSIAN PROTOTYPE FILTERS

Zero-phase filters, in particular Gaussian filters are often used in image processing because they have the useful feature to yield filtered images free of any phase distortions. We begin our design with the 1D Gaussian prototype filter function in the frequency domain:

$$G(\omega) = \exp\left(-\sigma^2\omega^2/2\right). \tag{1}$$

For simplicity, instead of (1), we use the expression $G_P(\omega) = \exp\left(-p^2\cdot\omega^2\right)$, with $p = \sigma/\sqrt{2}$, where p has the role of a selectivity parameter; the larger the value of p, the narrower will be the Gaussian. The design procedure presented next relies on a polynomial approximation of the 1D Gaussian prototype $\exp\left(-p^2\omega^2\right)$. One of the most efficient rational approximations (with best tradeoff between accuracy and order) is given by Chebyshev-Padé method, which yields a uniform approximation of a function over a specified range. Its single drawback is that its coefficients can only be derived numerically, using a symbolic calculation software like MAPLE. Since we need a parametric (adjustable) 2D filter with specified parameters, we first obtain a rational approximation of Gaussian $G_0(\omega) = \exp(-\omega^2)$, taking $p = 1$. The following approximation results, accurate on a frequency range much larger than $[-\pi, \pi]$, this being essential for our purpose:

$$G_0(\omega) \cong 0.01617\cdot\left(\omega^4 - 18.618\cdot\omega^2 + 84.27525\right)/\left(\omega^4 + 0.466737\cdot\omega^2 + 1.362717\right). \tag{2}$$

The derived approximation (2) is scalable of the frequency axis, i.e. substituting the current variable ω by $p\cdot\omega$ ($p > 0$), the approximation remains valid for a certain range of the scaling parameter p. For a value of the parameter p different from unity, the characteristic $G_0(\omega)$ either stretches (for $p < 1$) or shrinks (for $p > 1$). Thus the 1D Gaussian filter becomes parametric depending on p. Therefore, approximation (2) can be written for the parametric Gaussian $G_P(\omega) = \exp\left(-p^2\cdot\omega^2\right)$, where $\xi = 0.01617$:

$$G_P(\omega) = \exp\left(-p^2\cdot\omega^2\right) \cong \xi\cdot\frac{\left(p^4\cdot\omega^4 - 18.618\cdot p^2\cdot\omega^2 + 84.27525\right)}{\left(p^4\cdot\omega^4 + 0.466737\cdot p^2\cdot\omega^2 + 1.362717\right)} = \xi\cdot\frac{P_P(\omega)}{Q_P(\omega)}. \tag{3}$$

In the design it would be useful to find the value of the scaling parameter p which corresponds to a specified filter bandwidth. As in the case of common filters, we impose a desired cut-off frequency (–3dB bandwidth) ω_c and we obtain the value of p to be imposed:

$$G_P(\omega_c) = \exp\left(-p^2\cdot\omega_c^2\right) = 1/\sqrt{2} \quad \Rightarrow \quad p = \sqrt{\ln\sqrt{2}}/\omega_c \cong 0.5887/\omega_c. \tag{4}$$

The Gaussian approximation $G_P(\omega)$ is plotted in Fig. 1a for various values of scaling parameter p. Starting from (3), a band-pass (BP) Gaussian filter results by summing two Gaussians shifted to $-\omega_0$ and ω_0:

$$G_{BP}(\omega) = \exp\left(-p^2\cdot(\omega-\omega_0)^2\right) + \exp\left(-p^2\cdot(\omega+\omega_0)^2\right), \tag{5}$$

where ω_0 is the peak frequency of the BP filter. Its frequency response, using (3), can be written as:

$$G_{BP}(\omega) = \xi\cdot\frac{P_P(\omega-\omega_0)}{Q_P(\omega-\omega_0)} + \xi\cdot\frac{P_P(\omega+\omega_0)}{Q_P(\omega+\omega_0)} = \xi\cdot\frac{P_P(\omega-\omega_0)\cdot Q_P(\omega+\omega_0) + P_P(\omega+\omega_0)\cdot Q_P(\omega-\omega_0)}{Q_P(\omega-\omega_0)\cdot Q_P(\omega+\omega_0)}. \tag{6}$$

Substituting now the shifted numerator $P_P(\omega\pm\omega_0)$ and denominator $Q_P(\omega\pm\omega_0)$ from (3) into expression (6), after performing the calculations, finally the frequency response $G_{BP}(\omega)$ of the Gaussian BP filter results as the ratio of the following two parametric even polynomials of degree 8, written in descending powers of the frequency variable ω as:

$$G_{BP}(\omega)=\xi\cdot\frac{\left(\begin{array}{l}2p^8\cdot\omega^8-p^6\cdot\left(8p^2\omega_0^2+36.3025\right)\cdot\omega^6+p^4\left(12\,p^4\omega_0^4+36.3025\cdot p^2\omega_0^2+153.8965\right)\cdot\omega^4\\+\left(-8p^8\omega_0^6+36.302526\,p^6\omega_0^4+1062.41447\,p^4\omega_0^2+27.9266267\,p^2\right)\cdot\omega^2\\+2p^8\cdot\omega_0^8-36.302526\,p^6\omega_0^6+153.89652\,p^4\omega_0^4+27.9266267\,p^2\omega_0^2+229.686638\end{array}\right)}{\left(\begin{array}{l}p^8\cdot\omega^8+\left(-4p^8\omega_0^2+0.933474\,p^6\right)\cdot\omega^6+p^4\left(6\,p^4\omega_0^4-0.933474\cdot p^2\omega_0^2+2.943277\right)\cdot\omega^4\\+\left(-4p^8\omega_0^6-0.933474\,p^6\omega_0^4+15.916917\,p^4\omega_0^2+1.272061\,p^2\right)\cdot\omega^2\\+p^8\omega_0^8+0.933474\,p^6\omega_0^6+2.943277\,p^4\omega_0^4+1.272061\,p^2\omega_0^2+1.85699\end{array}\right)}=\xi\cdot\frac{G_N(\omega)}{G_D(\omega)} \tag{7}$$

where the numerator $G_N(\omega)$ and the denominator $G_D(\omega)$ are even order polynomials of the form:

$$G_N(\omega)=a_4\cdot\omega^8+a_3\cdot\omega^6+a_2\cdot\omega^4+a_1\cdot\omega^2+a_0\ ;\qquad G_D(\omega)=b_4\cdot\omega^8+b_3\cdot\omega^6+b_2\cdot\omega^4+b_1\cdot\omega^2+b_0. \tag{8}$$

The coefficients of the above polynomials are found by simple identification and have the following expressions depending on the scaling parameter *p* and the specified peak frequency ω_0 of the BP prototype:

$$\begin{array}{l}a_4=2p^8;\quad a_3=-p^6(8p^2\cdot\omega_0^2+36.30253);\quad a_2=p^4\cdot(12p^4\cdot\omega_0^4+36.30253\cdot p^2\cdot\omega_0^2+153.89652);\\a_1=p^2\cdot(27.92663+1062.41447\cdot p^2\cdot\omega_0^2+36.30253\cdot p^4\cdot\omega_0^4-8\cdot p^6\cdot\omega_0^6);\\a_0=2p^8\cdot\omega_0^8-36.30253\cdot p^6\cdot\omega_0^6+153.89652\cdot p^4\cdot\omega_0^4+27.926627\cdot p^2\cdot\omega_0^2+229.68664;\\b_4=p^8;\quad b_3=p^6(-4p^2\cdot\omega_0^2+0.933474)\qquad b_2=p^4\cdot(6p^4\cdot\omega_0^4-0.933474\cdot p^2\cdot\omega_0^2+2.943277);\\b_1=p^2\cdot(1.272061+15.916917\cdot p^2\cdot\omega_0^2-0.933474\cdot p^4\cdot\omega_0^4-4\cdot p^6\cdot\omega_0^6);\\b_0=p^8\cdot\omega_0^8+0.933474\cdot p^6\cdot\omega_0^6+2.943277427\cdot p^4\cdot\omega_0^4+1.272061\cdot p^2\cdot\omega_0^2+1.856997622.\end{array} \tag{9}$$

Thus, for any specified selectivity given by the scaling parameter *p* and a central frequency ω_0, the BP filter coefficients are determined directly determined using relations (9).

Two examples are given as follows. For the specifications $\omega_0=\pi/3$, $p=9$, we get the following frequency response of the band-pass prototype, where $k=0.03234$ (shown in Fig. 1b):

$$G_{BP1}(\omega)=k\cdot\frac{\left(\omega^4-1.199345\cdot\omega^2+0.389249\right)\left(\omega^4-3.411237\cdot\omega^2+2.992464\right)}{\left(\omega^4-1.869429\cdot\omega^2+0.906318\right)\left(\omega^4-2.505538\cdot\omega^2+1.613057\right)} \tag{10}$$

For $\omega_0=\pi/2$, $p=3$ we get the BP frequency response, with the same constant, $k=0.03234$:

$$G_{BP2}(\omega)=k\cdot\frac{\left(\omega^2-0.217439\right)\left(\omega^2-1.304327\right)\left(\omega^4+1.521766\cdot\omega^2+44.486768\right)}{\left(\omega^4-0.01376\cdot\omega^2+0.0107423\right)\left(\omega^4-9.752127\cdot\omega^2+36.163913\right)}. \tag{11}$$

An important remark regarding the BP Gaussian prototype $G_{BP}(\omega)$ given by (7) is that it is parametric, depending on the scaling parameter p and the specified peak frequency ω_0. For certain limits of variation of the scaling parameter *p*, within which the approximation (3) remains valid, we can obtain various BP prototypes, all of them of the same order of complexity, in our case $N=8$. As we will see in the following section, this prototype will generate a very efficient 2D elliptically-shaped filter.

3. ANALYTICAL DESIGN METHOD FOR ELLIPTICALLY-SHAPED FILTERS

In this section, 2D elliptical filters will be derived by applying a specific frequency transformation to a factored polynomial approximation of the prototype frequency response.

3.1. Frequency mapping for designing elliptically-shaped filters

The specified parameters are the values of the ellipse semi-axes and the orientation, described by the angle formed by the large axis with frequency axis ω_1. From the frequency response (3) of the 1D prototype filter, we obtain a 2D filter with elliptical shape using the frequency mapping $\omega^2 \to E_\varphi(\omega_1,\omega_2)$, where [17]:

$$E_\varphi(\omega_1,\omega_2)=\omega_1^2\left(\frac{\cos^2\varphi}{E^2}+\frac{\sin^2\varphi}{F^2}\right)+\omega_2^2\left(\frac{\sin^2\varphi}{E^2}+\frac{\cos^2\varphi}{F^2}\right)+\omega_1\omega_2\sin(2\varphi)\left(\frac{1}{F^2}-\frac{1}{E^2}\right)=a_0\cdot\omega_1^2+b_0\cdot\omega_2^2+c_0\cdot\omega_1\omega_2 \quad (12)$$

The mapping of a circular filter into an elliptical filter is described by a linear frequency transformation [16]:

$$\begin{bmatrix}\omega_1\\ \omega_2\end{bmatrix}=\begin{bmatrix}E & 0\\ 0 & F\end{bmatrix}\cdot\begin{bmatrix}\cos\varphi & -\sin\varphi\\ \sin\varphi & \cos\varphi\end{bmatrix}\cdot\begin{bmatrix}\omega_1'\\ \omega_2'\end{bmatrix}, \quad (13)$$

where usually $E>F$; in (13), (ω_1,ω_2) are the transformed variables and (ω_1',ω_2') are the former variables. In this way, the unit circle is dilated along the axes ω_1,ω_2 with factors *E* and *F*, then rotated with angle φ, thus turning into a tilted ellipse. Thus, starting from a 1D prototype, a 2D elliptical filter results, described by parameters *E*, *F* and φ. Using the identity $\omega_1\omega_2=0.5\cdot\left((\omega_1+\omega_1)^2-\omega_1^2-\omega_2^2\right)$, we get the mapping:

$$\omega^2 \to E_\varphi(\omega_1,\omega_2)=a\cdot\omega_1^2+b\cdot\omega_2^2+c\cdot(\omega_1+\omega_2)^2. \quad (14)$$

With notations $q=1/E^2+1/F^2$, $r=1/E^2-1/F^2$, the expressions of coefficients *a*, *b* and *c* result as:

$$\begin{aligned}a&=a_0-0.5c_0=q+r\cdot\cos(2\varphi)+r\cdot\sin(2\varphi)\\ b&=b_0-0.5c_0=q-r\cdot\cos(2\varphi)+r\cdot\sin(2\varphi)\\ c&=0.5c_0=-r\cdot\sin(2\varphi).\end{aligned} \quad (15)$$

To find a rational trigonometric approximation for ω^2 on the range $[-\pi,\pi]$, we use the variable change [14]:

$$\omega=\arccos(x/\pi) \;\leftrightarrow\; x=\pi\cos\omega. \quad (16)$$

First we will find a rational approximation for the function $\left(\arccos(x/\pi)\right)^2$, using the change of variable (16). Thus, we obtain the first-order Chebyshev-Padé approximation in *x*:

$$\left(\arccos(x/\pi)\right)^2\cong\left(2.357533-0.710425\cdot x\right)/\left(1+0.147456\cdot x\right). \quad (17)$$

Substituting back in (17) $x=\pi\cos\omega$, we get the following approximation for ω^2, plotted in Fig. 1c:

$$\omega^2\cong 2.357533\cdot\left(1-0.946216\cdot\cos\omega\right)/\left(1+0.463012\cdot\cos\omega\right)=P(\omega)/Q(\omega). \quad (18)$$

This approximation turns out to be accurate for $\omega\in[-\pi,\pi]$, with visible errors only near the margins of the specified frequency range, where it diverges; being of minimum order, it is also very efficient. An even more accurate approximation of ω^2, derived similarly, given by the second-order expression:

$$\omega^2\cong 1.3451\cdot\left(1-0.31518\cdot\cos\omega-0.68117\cdot\cos 2\omega\right)/\left(1+0.99346\cdot\cos\omega+0.08573\cdot\cos 2\omega\right) \quad (19)$$

shown in Fig. 1d. Obviously, the second approximation will give in principle 2D filters with a more accurate shape, but their order of complexity will be double. Therefore, we will mainly use in our design the first-order approximation, and the second one will be eventually used only when the first one gives very large distortions in shape. Writing the approximation (18) for the two frequency variables ω_1, ω_2 and their sum $\omega_1+\omega_2$ respectively, the expressions of ω_1^2, ω_2^2 and $(\omega_1+\omega_2)^2$ are then replaced into (14)

$$\omega^2 \to E_\varphi(\omega_1,\omega_2)=a\cdot\frac{P(\omega_1)}{Q(\omega_1)}+b\cdot\frac{P(\omega_2)}{Q(\omega_2)}+c\cdot\frac{P(\omega_1+\omega_2)}{Q(\omega_1+\omega_2)}=\frac{M(\omega_1,\omega_2)}{N(\omega_1,\omega_2)}. \quad (20)$$

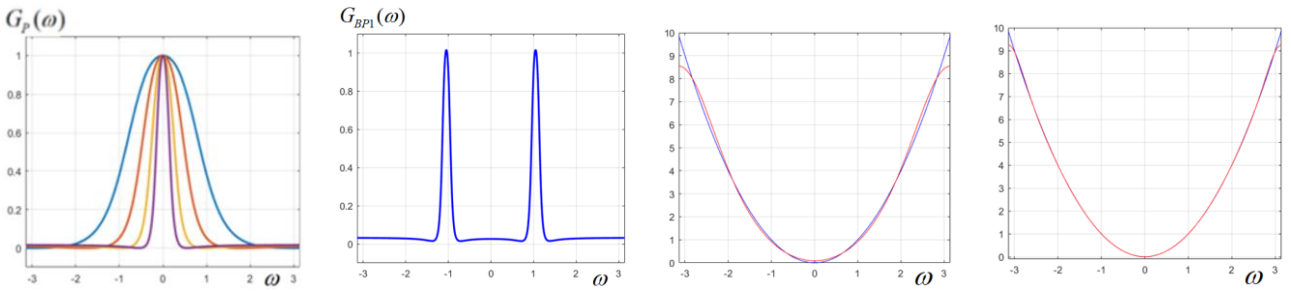

(a) (b) (c) (d)

Fig. 1 – a) Prototype function $G_P(\omega)$ for: $p=1$ (blue), $p=1.7$ (red), $p=3$ (orange), $p=6$ (magenta); b) BP filter $G_{BP1}(\omega)$; c) first-order approximation of function ω^2; d) second-order approximation of function ω^2.

Making the calculations and using trigonometric identities we obtain the numerator and denominator as:

$$M(\omega_1,\omega_2)=a\cdot P(\omega_1)\cdot Q(\omega_2)\cdot Q(\omega_1+\omega_2)+b\cdot Q(\omega_1)\cdot P(\omega_2)\cdot Q(\omega_1+\omega_2)+c\cdot Q(\omega_1)\cdot Q(\omega_2)\cdot P(\omega_1+\omega_2) \quad (21)$$

$$N(\omega_1,\omega_2)=Q(\omega_1)\cdot Q(\omega_2)\cdot Q(\omega_1+\omega_2). \quad (22)$$

Substituting the expressions $P(\omega)$, $Q(\omega)$ from (18) in (21), the parametric numerator $M(\omega_1,\omega_2)$ results as:

$$\begin{aligned}M(\omega_1,\omega_2)&=q\cdot M_0(\omega_1,\omega_2)+r\cdot(\cos 2\varphi)\cdot M_1(\omega_1,\omega_2)+r\cdot(\sin 2\varphi)\cdot M_2(\omega_1,\omega_2)=\\&=q\cdot\begin{pmatrix}4.47596-1.4029\cos\omega_1-1.4029\cos\omega_2+1.15024\cos(\omega_1+\omega_2)-1.0328\cos(\omega_1-\omega_2)-0.2391\cos 2\omega_1\\-0.2391\cos 2\omega_2-0.26372\cos(\omega_1+2\omega_2)-0.26372\cos(2\omega_1+\omega_2)-0.2391\cos(2\omega_1+2\omega_2)\end{pmatrix}\\&+\left(-2.553164\cos\omega_1+2.553164\cos\omega_2+0.769105\cos(\omega_1+2\omega_2)-0.769105\cos(2\omega_1+\omega_2)\right)\cdot r\cdot\cos 2\varphi\\&+\begin{pmatrix}2.23798-1.97804\cos\omega_1-1.97804\cos\omega_2+3.128286\cos(\omega_1+\omega_2)-1.28552\cos(\omega_1-\omega_2)\\-0.11955\cos 2\omega_1-0.11955\cos 2\omega_2+0.252691\cos(\omega_1+2\omega_2)+0.252691\cos(2\omega_1+\omega_2)\\-0.11955\cos(2\omega_1+2\omega_2).\end{pmatrix}\cdot r\cdot\sin 2\varphi\end{aligned} \quad (23)$$

Similarly, the denominator $N(\omega_1,\omega_2)$ is obtained from (22) as:

$$\begin{aligned}N(\omega_1,\omega_2)=&1.024813+0.570184\cos\omega_1+0.570184\cos\omega_2+0.570184\cos(\omega_1+\omega_2)\\&+0.107184\cos(\omega_1-\omega_2)+0.024813\cos 2\omega_1+0.024813\cos 2\omega_2+0.107184\cos(\omega_1+2\omega_2)\\&+0.107184\cos(2\omega_1+\omega_2)+0.024813\cos(2\omega_1+2\omega_2).\end{aligned} \quad (24)$$

Using trigonometric identities $\cos\omega_1=0.5\cdot(z_1+z_1^{-1})$, $\cos\omega_2=0.5\cdot(z_2+z_2^{-1})$, in complex frequency variables $z_1=e^{j\omega_1}$, $z_2=e^{j\omega_2}$ and taking into account (18) and (20)–(22), the mapping (20) is expressed in matrix form:

$$\omega^2\rightarrow\left(\mathbf{z}_1\times\mathbf{M}\times\mathbf{z}_2^T\right)\Big/\left(\mathbf{z}_1\times\mathbf{N}\times\mathbf{z}_2^T\right), \quad (25)$$

where the vectors are: $\mathbf{z}_1=[1\quad z_1^{-1}\quad\ldots\quad z_1^{-4}]$ and $\mathbf{z}_2=[1\quad z_2^{-1}\quad\ldots\quad z_2^{-4}]$. The matrix corresponding to the numerator $M(\omega_1,\omega_2)$ in (16) is given by the linear combination of matrices:

$$\mathbf{M}=q\cdot\mathbf{M}_0+r\cdot(\cos 2\varphi)\cdot\mathbf{M}_1+r\cdot(\sin 2\varphi)\cdot\mathbf{M}_2, \quad (26)$$

where the component matrices $\mathbf{M}_0$, $\mathbf{M}_1$ and $\mathbf{M}_2$ of size 5×5 have constant elements and result by identifying the corresponding coefficients from the terms $M_0(\omega_1,\omega_2)$, $M_1(\omega_1,\omega_2)$ and $M_2(\omega_1,\omega_2)$ of (23), interpreted as Discrete Space Fourier Transforms (DSFT) of the matrices $\mathbf{M}_0$, $\mathbf{M}_1$ and $\mathbf{M}_2$, respectively. The denominator $N(\omega_1,\omega_2)$ also corresponds to a 5×5 matrix $\mathbf{N}$ with constant elements, resulted similarly through identifying coefficients of the terms of $N(\omega_1,\omega_2)$ in (24), regarded as DSFT.

$$\mathbf{M}_0=\begin{bmatrix} 0 & 0 & -0.1196 & -0.1318 & -0.1196 \\ 0 & -0.5164 & -0.7015 & 0.5751 & -0.1318 \\ -0.1196 & -0.7015 & 4.4760 & -0.7015 & -0.1196 \\ -0.1318 & 0.5751 & -0.7015 & -0.5164 & 0 \\ -0.1196 & -0.1318 & -0.1196 & 0 & 0 \end{bmatrix};\quad \mathbf{M}_1=\begin{bmatrix} 0 & 0 & 0 & 0.3846 & 0 \\ 0 & 0 & 1.2766 & 0 & -0.3846 \\ 0 & -1.2766 & 0 & -1.2766 & 0 \\ -0.3846 & 0 & 1.2766 & 0 & 0 \\ 0 & 0.3846 & 0 & 0 & 0 \end{bmatrix} \tag{27}$$

$$\mathbf{M}_2=\begin{bmatrix} 0 & 0 & -0.0598 & 0.1264 & -0.0598 \\ 0 & -0.6429 & -0.9890 & 1.5642 & 0.1264 \\ -0.0598 & -0.9890 & 2.2380 & -0.9890 & -0.0598 \\ 0.1264 & 1.5642 & -0.9890 & -0.6429 & 0 \\ -0.0598 & 0.1264 & -0.0598 & 0 & 0 \end{bmatrix};\quad \mathbf{N}=\begin{bmatrix} 0 & 0 & 0.0124 & 0.0536 & 0.0124 \\ 0 & 0.0536 & 0.2851 & 0.2851 & 0.0536 \\ 0.0124 & 0.2851 & 1.0248 & 0.2851 & 0.0124 \\ 0.0536 & 0.2851 & 0.2851 & 0.0536 & 0 \\ 0.0124 & 0.0536 & 0.0124 & 0 & 0 \end{bmatrix} \tag{28}$$

As can be noticed, the matrices $\mathbf{M}_0$, $\mathbf{M}_1$, $\mathbf{M}_2$ and $\mathbf{N}$ have a "band" structure along the second diagonal and are symmetric with respect to the central element. Once specified the semi-axes E and F of the ellipse and the orientation angle φ, the matrix $\mathbf{M}$ is determined from (26), using (27)–(28). The elements of the 5×5 matrices $\mathbf{M}$ and $\mathbf{N}$ are obtained by identifying terms of the expressions $M(\omega_1,\omega_2)$ and $N(\omega_1,\omega_2)$ as terms of Discrete Space Fourier Transform (DSFT) in frequency variables ω_1 and ω_2.

3.2. Frequency response of the elliptically-shaped filter

The next step of the proposed design method is to apply the frequency transformation (25) to the low-pass or band-pass prototype filter. As shown in section 2, the BP prototype of order 8 generally expressed as:

$$H_P(\omega)=\left(a_4\cdot\omega^8+a_3\cdot\omega^6+a_2\cdot\omega^4+a_1\cdot\omega^2+a_0\right)\Big/\left(b_4\cdot\omega^8+b_3\cdot\omega^6+b_2\cdot\omega^4+b_1\cdot\omega^2+b_0\right) \tag{29}$$

can always be factored at least into two fractions, each one with the general expression:

$$H_{Pi}(\omega)=\gamma\cdot\left(\omega^4+\alpha_1\cdot\omega^2+\alpha_0\right)\Big/\left(\omega^4+\beta_1\cdot\omega^2+\beta_0\right). \tag{30}$$

Applying the frequency mapping (25) to this prototype factor, we get directly the frequency response or transfer function of the corresponding 2D elliptically-shaped filter factor:

$$H_{B1}(z_1,z_2)=\left(\mathbf{z}_1\times\mathbf{A}_1\times\mathbf{z}_2^T\right)\Big/\left(\mathbf{z}_1\times\mathbf{B}_2\times\mathbf{z}_2^T\right) \tag{31}$$

where $\times$ is inner product and the vectors are: $\mathbf{z_1}=[1\quad z_1^{-1}\quad z_1^{-2}\quad \ldots\quad z_1^{-8}]$, $\mathbf{z_2}=[1\quad z_2^{-1}\quad z_2^{-2}\quad \ldots\quad z_2^{-8}]$. The 9×9 matrices $\mathbf{A}_1$ and $\mathbf{B}_1$ result as a weighted sum of convolutions of the 5×5 matrices $\mathbf{M}$ and $\mathbf{N}$:

$$\mathbf{A}_1=\mathbf{M}*\mathbf{M}+\alpha_1\cdot\mathbf{M}*\mathbf{N}+\alpha_0\cdot\mathbf{N}*\mathbf{N};\qquad \mathbf{B}_1=\mathbf{M}*\mathbf{M}+\beta_1\cdot\mathbf{M}*\mathbf{N}+\beta_0\cdot\mathbf{N}*\mathbf{N}. \tag{32}$$

Thus, the pairs of matrices $(\mathbf{A}_1,\mathbf{B}_1)$, $(\mathbf{A}_2,\mathbf{B}_2)$ are calculated for the two factors $H_{B1}(\omega)$, $H_{B2}(\omega)$ and the matrices $\mathbf{A}_E$, $\mathbf{B}_E$ of the overall elliptical filter $H_E(z_1,z_2)=A_E(z_1,z_2)/B_E(z_1,z_2)$ also result by convolution:

$$\mathbf{A}_E=\mathbf{A}_1*\mathbf{A}_2;\qquad \mathbf{B}_E=\mathbf{B}_1*\mathbf{B}_2. \tag{33}$$

In (32) and (33) the symbol $*$ means two-dimensional convolution of matrices. In our case, by convolving matrices of size $N\times N$, we get a $(2N-1)\times(2N-1)$ matrix. The same applies to equations (38) and (39). As a remark, even if the filter transfer function $H_E(z_1,z_2)$ is expressed in the complex frequency variables z_1 and z_2 to be conveniently put in matrix form, it is a real number, so the obtained 2D filter is *zero-phase*.

3.3. Circular filters derived as a particular case

A useful particular case of the designed elliptically-shaped filters are obviously the circular filters. They can be obtained using a particular choice of parameters in frequency mapping (11), namely equal semi-axes $E=F=\sqrt{2}$ and orientation angle of arbitrary value, in particular $\varphi=0$. With these settings, the

transformation (14) becomes $\omega^2 \to \omega_1^2 + \omega_2^2$, which is known to yield circularly-shaped filters. The mapping (12) in principle remains valid, and since in (15) we have $q=1$, $r=0$, the matrix $\mathbf{M}$ reduces to the 5×5 constant matrix $\mathbf{M}_0$. However, through a direct analysis of the circular case, the designed filter may result less complex. Thus, writing (18) for frequency variables ω_1 and ω_2, we obtain:

$$\omega^2 \to 2.35753 \cdot \left[\frac{1-0.946216\cos\omega_1}{1+0.46301\cdot\cos\omega_1} + \frac{1-0.946216\cos\omega_2}{1+0.46301\cdot\cos\omega_2} \right] = \frac{M_C(\omega_1,\omega_2)}{N_C(\omega_1,\omega_2)}. \tag{34}$$

Using trigonometric identities as before, the mapping (34) in matrix form will be:

$$\omega^2 \to M_C(\omega_1,\omega_2)/N_C(\omega_1,\omega_2) = \left(\mathbf{z}_1 \times \mathbf{M}_C \times \mathbf{z}_2^T\right) \Big/ \left(\mathbf{z}_1 \times \mathbf{N}_C \times \mathbf{z}_2^T\right), \tag{35}$$

where the vectors are: $\mathbf{z_1} = [1 \;\; z_1^{-1} \;\; z_1^{-2}]$; $\mathbf{z_2} = [1 \;\; z_2^{-1} \;\; z_2^{-2}]$. The numerator $M_C(\omega_1,\omega_2)$ and denominator $N_C(\omega_1,\omega_2)$ are in fact the Discrete Space Fourier Transforms (DSFT) of the matrices $\mathbf{M}_C$ and $\mathbf{N}_C$:

$$\mathbf{M}_C = \begin{bmatrix} -0.4366 & -0.7618 & -0.4366 \\ -0.7618 & 4.7938 & -0.7618 \\ -0.4366 & -0.7618 & -0.4366 \end{bmatrix}, \qquad \mathbf{N}_C = \begin{bmatrix} 0.03317 & 0.18214 & 0.03317 \\ 0.18214 & 1 & 0.18214 \\ 0.03317 & 0.18214 & 0.03317 \end{bmatrix} \tag{36}$$

Once found the frequency mapping for circular filters, the next steps of the design process are similar to those for elliptical filters, described in sub-section 3.2. Based on the Gaussian BPF prototype given by (29), factored into two ratios like (30) and applying the frequency mapping (35), we obtain the transfer function of the corresponding 2D circular filter factor:

$$H_{BC1}(z_1, z_2) = \left(\mathbf{z}_1 \times \mathbf{A}_{C1} \times \mathbf{z}_2^T\right) \Big/ \left(\mathbf{z}_1 \times \mathbf{B}_{C2} \times \mathbf{z}_2^T\right), \tag{37}$$

where $\times$ is inner product and the vectors are: $\mathbf{z_1} = [1 \;\; z_1^{-1} \;\; z_1^{-2} \;\; \ldots \;\; z_1^{-4}]$, $\mathbf{z_2} = [1 \;\; z_2^{-1} \;\; z_2^{-2} \;\; \ldots \;\; z_2^{-4}]$. The 5×5 matrices $\mathbf{A}_{C1}$ and $\mathbf{B}_{C1}$ result as a weighted sum of convolutions of the 3×3 matrices $\mathbf{M}_C$, $\mathbf{N}_C$:

$$\mathbf{A}_{C1} = \mathbf{M}_C * \mathbf{M}_C + \alpha_1 \cdot \mathbf{M}_C * \mathbf{N}_C + \alpha_0 \cdot \mathbf{N}_C * \mathbf{N}_C \;; \quad \mathbf{B}_{C1} = \mathbf{M}_C * \mathbf{M}_C + \beta_1 \cdot \mathbf{M}_C * \mathbf{N}_C + \beta_0 \cdot \mathbf{N}_C * \mathbf{N}_C . \tag{38}$$

Determining similarly the 5×5 matrices $\mathbf{A}_{C2}$ and $\mathbf{B}_{C2}$ for the second factor, the matrices $\mathbf{A}_C$ and $\mathbf{B}_C$ of the overall elliptical filter $H_C(z_1, z_2) = A_C(z_1, z_2)/B_C(z_1, z_2)$ also result by convolution, and are of size 9×9:

$$\mathbf{A}_C = \mathbf{A}_{C1} * \mathbf{A}_{C2} \;; \qquad \mathbf{B}_C = \mathbf{B}_{C1} * \mathbf{B}_{C2} . \tag{39}$$

Thus, designing circular filters directly rather than as a particular elliptical filter, complexity is much lower.

3.4. Design algorithm

The design procedure described above is presented in a brief, synthetic form as follows. Since the proposed design method is analytical, there is no optimization procedure and therefore no iterative algorithm seeking to minimize a cost function or error (such as LMS, RLS etc.). However, the sequence of design steps presented as follows can be regarded as an associated pseudo-code:

For elliptically-shaped band-pass filters:

(a) Calculate the parameters q and r, from the specified semiaxes values, *E* and *F*;
(b) Read the matrices $\mathbf{M}_0$, $\mathbf{M}_1$, $\mathbf{M}_2$ and $\mathbf{N}$ with fixed, constant elements from (27)–(28);
(c) Calculate $\cos 2\varphi$ and $\sin 2\varphi$, from the specified orientation angle φ;
(d) Calculate the frequency mapping matrix $\mathbf{M}$ using (26);
(e) Calculate the scaling parameter *p*, from the specified bandwidth or cutoff frequency ω_c, using (4);
(f) Calculate using (9) the set of coefficients $a_0,...,a_4$, $b_0,...,b_4$, for given p and peak frequency ω_0.
(g) The Gaussian BPF prototype is factored into two elementary fractions like (30), as in examples (10) and (11), thus their coefficients are determined;
(h) Determine matrices $\mathbf{A}_1$, $\mathbf{B}_1$ for the two factor fractions, using (32) and coefficients from step (g);

(i) Finally, calculate the matrices $\mathbf{A}_E$ and $\mathbf{B}_E$ of the overall elliptical filter using (33).

For circular band-pass filters:

(a) Calculate the scaling parameter p using (4), from the specified bandwidth or cutoff frequency ω_c;

(b) Calculate using (9) the set of coefficients $a_0,...,a_4$, $b_0,...,b_4$, for given p and peak frequency ω_0.

(c) The Gaussian BPF prototype is factored into two elementary fractions like (30), as in examples (10) and (11), thus their coefficients are determined;

(d) Read the matrices $\mathbf{M}_C$ and $\mathbf{N}_C$ with fixed, constant elements (from (36));

(e) Determine matrices $\mathbf{A}_{C1}$, $\mathbf{B}_{C1}$ for the two factor fractions, using (38) and coefficients from step (c);

(f) Determine the matrices $\mathbf{A}_C$ and $\mathbf{B}_C$ of the overall circular filter using (39).

The functions written in MATLAB implementing these pseudocodes, which calculate and plot the frequency response and contour plot for any given specifications can be found in the repository webpage [20].

3.5. Design examples of elliptical and circular filters

Next, some design examples are given for various elliptical and circular filters with imposed specifications, using the proposed analytical technique. In Fig. 2 the frequency responses and corresponding contour plots are displayed for 6 elliptical filters, described by the given parameter values (peak frequency ω_0, scaling parameter p, semi-axes E and F, orientation angle φ). The filter (a) is a very selective LP elliptical filter, the rest are BP filters. As can be noticed, all filters have an accurate elliptical shape in the frequency plane, without visible distortions even near the margins.

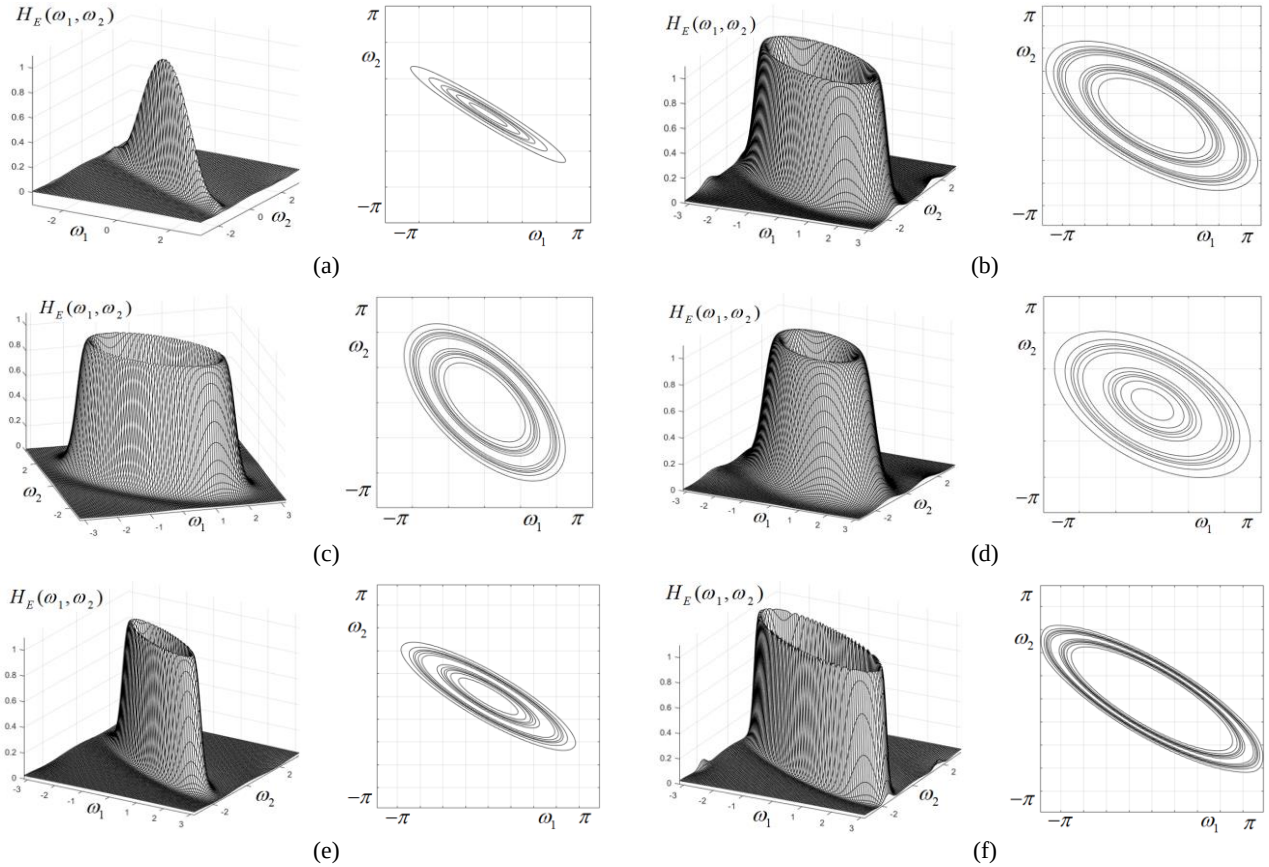

Fig. 2 – Frequency responses and contour plots for the given parameter values: a) $p=9$, $E=3$, $F=0.3$, $\varphi=\pi/6$; b) $\omega_0=\pi/2$, $p=3$, $E=2.3$, $F=1$, $\varphi=\pi/6$; c) $\omega_0=\pi/2$, $p=3$, $E=2$, $F=1$, $\varphi=\pi/4$; d) $\omega_0=\pi/4$, $p=3$, $E=3.4$, $F=1.8$, $\varphi=\pi/6$; e) $\omega_0=\pi/4$, $p=4$, $E=3.4$, $F=0.8$, $\varphi=\pi/6$; f) $\omega_0=\pi/2$, $p=6$, $E=2.8$, $F=0.8$, $\varphi=\pi/6$.

Some examples of circular BP Gaussian filters designed using the given specifications are shown in Fig. 3. The filters (a) and (b) are obtained using the simpler, first-order approximation (18); while the narrower filter (with $\omega_0 = \pi/3$) has a good circular shape, the wider filter (for $\omega_0 = 3\pi/4$), as show the contours, has a shape with some visible distortions from circularity. This effect is more visible for wider filters, i.e. towards the frequency plane margins. For a correct shape, we should use the second-order approximation (19); thus we obtain the circular filters (c), (d), with peak frequency $\omega_0 = 0.8\pi$ and scaling parameter $p = 3$ and $p = 9$ respectively. This time, the contours show a very accurate circular shape even near frequency plane margins; of course, this shape accuracy comes with the price of a double order of complexity for the 2D filter.

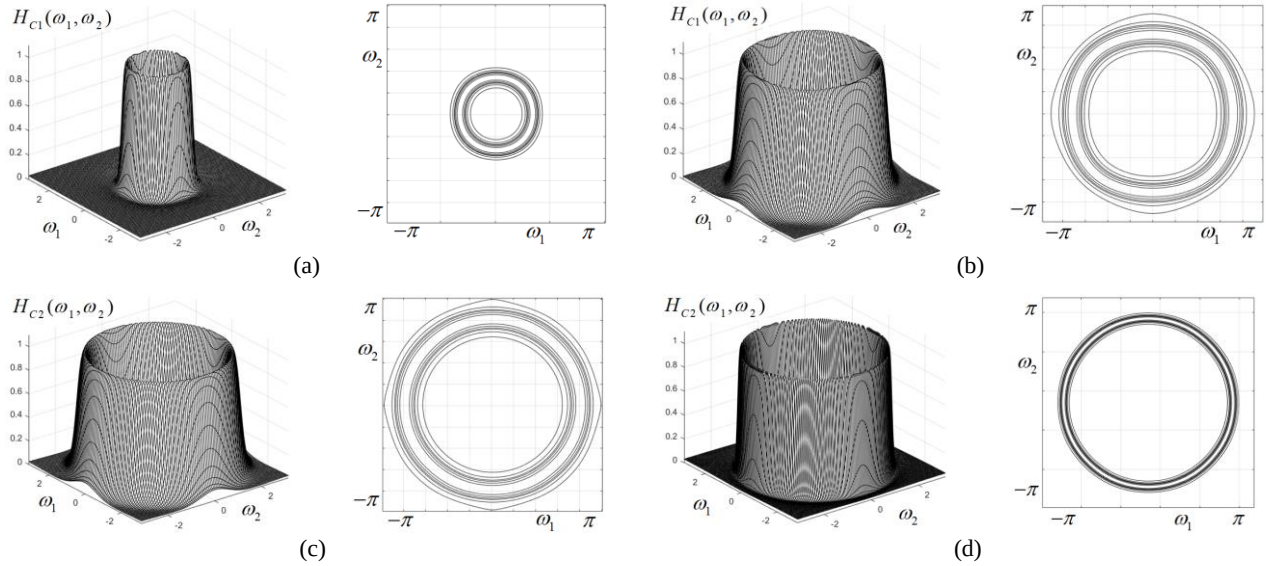

Fig. 3 – Frequency responses and contour plots of circular filters for the given parameter values: a) $\omega_0 = \pi/3$, $p = 6$; b) $\omega_0 = 3\pi/4$, $p = 3$; c) $\omega_0 = 0.8\pi$, $p = 3$; d) $\omega_0 = 0.8\pi$, $p = 9$.

4. APPLICATIONS IN IMAGE FILTERING

Some simulation results are given here for image filtering applications of the designed elliptical and circular filters. First the FFT spectra of some simple binary test images are calculated and displayed, for a better understanding of their filtering. For instance, in Fig. 4, image (a) containing one black circle against white background, has the FFT spectrum magnitude (b) with a concentric circular shape and cross-section (c); image (d) with concentric circles also has a similar spectrum shown in (e); The test image (f) containing circles of various sizes and thickness has the FFT spectrum (g) with a fine concentric structure; LP or BP circular filters with various peak frequencies and bandwidths will simply select circular portions of these spectra. Of course, for more complex images, the spectrum is also complicated and filtering can no longer be easily interpreted. Image (h) results applying a narrow, circular LPF with $p = 5$; the LPF has an isotropic blurring effect depending on value *p*; as can be noticed, the larger and thicker objects remain more or less visible, while the thinner ones are very blurred. Then, by thresholding with a given threshold value, we get a binary image in which some objects from original image are preserved, while others vanish (like thinner rings), depending on the degree of blurring and threshold value; thus, image (i) results from the blurred image (h) by applying a threshold of value $th = 0.36$. However, in order to apply this subunitary threshold, the filtered image pixel values must be first scaled within the range $[0,1]$. Therefore, this LPF can be used to select objects in images, according to their size. Image (j) is the result of circular BP filtering.

The next examples shown in Fig. 5 use directional elliptical filters, with given specifications.. Image (a) contains ellipses of various sizes and orientations; its FFT spectrum (b), at a closer look, reveals also a fine elliptical structure. Using the elliptical LPF in Fig. 3a with parameters $p = 9$, $E = 3$, $F = 0.4$, $\varphi = \pi/6$, we get image (c) in which the objects (ellipses) whose spectra overlap with the filter characteristic are preserved, while the others are more or less blurred, depending on their orientation. Rotating the elliptical

filter by $\pi/2$, i.e. for an angle $\varphi = 2\pi/3$, other ellipses are detected and the former ones are blurred, as in image (d). Finally image (e) results from the elliptical BPF in Fig. 2b. In this case, the filter passes the medium frequencies, while the components of low and high frequencies are removed. Another filtering example is a "real-life" grayscale image of 650×750 pixels, in Fig. 5f, showing a view of high buildings (skyscrapers) seen from ground level (also used as test image in [19]). This image contains straight lines oriented under various angles, marking the building structure, and is convenient for testing directional filtering. The images in Figs. 5g–5i result from selective directional filtering, using an elliptical LP filter, with $p = 6$ and various orientation angles ($\varphi = \pi/6$, 0.4π, -0.2π). The directional filtering effect is clearly visible; according to specified filter orientation, different straight lines representing contours or other details are outlined, while others are more or less blurred, each depending on its orientation. Therefore, this directional filtering can be applied in detecting and selecting objects with various orientations from images. The MATLAB function for image filtering using such filters, as well as the used test images are available at [20].

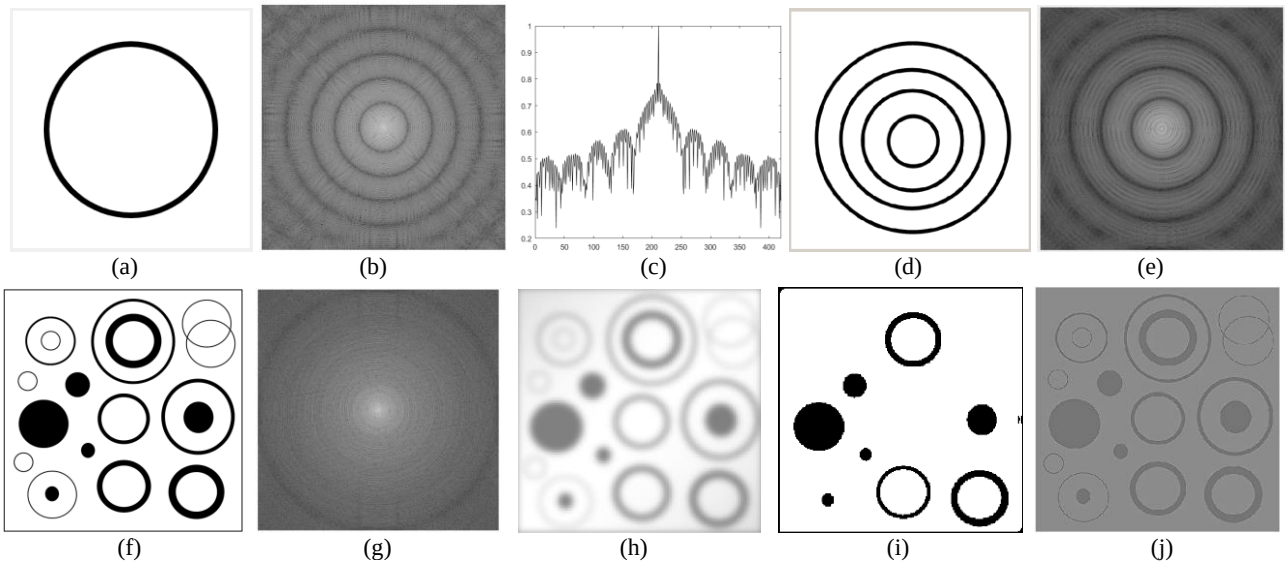

(a) (b) (c) (d) (e)

(f) (g) (h) (i) (j)

Fig. 4 a–d) Simple binary images containing circles; b–e) FFT spectrum magnitudes; c) cross-section of the FFT spectrum of image a); f) binary image with circles; g) its FFT spectrum; h) LP filtered image (p=5); i) image thresholded with $th = 0.36$; j) BP filtered image with $p = 5$, $\omega_0 = \pi/2$.

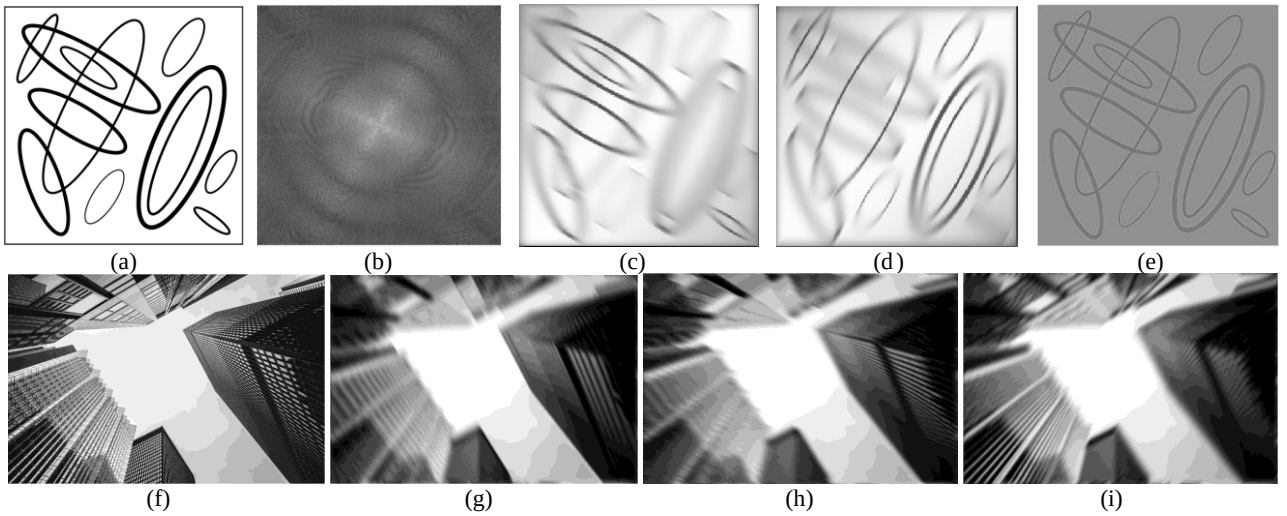

(a) (b) (c) (d) (e)

(f) (g) (h) (i)

Fig. 5 – a) Binary image with ellipses; b) its FFT spectrum; c) LP filtered with $p = 9$, $E = 3$, $F = 0.3$, $\varphi = \pi/6$; d) LP filtered with $p = 9$, $E = 3$, $F = 0.3$, $\varphi = 2\pi/3$; e) BP filtered with $\omega_0 = \pi/2$, $p = 3$, $E = 2.3$, $F = 1$, $\varphi = \pi/6$; f) skyscrapers image; g)–i) skyscraper image directionally filtered with $E = 6$, $F = 1$, $p = 6$ and angles: $\varphi = \pi/6$, $\varphi = 0.4\pi$, $\varphi = -0.2\pi$, respectively.

5. COMPARATIVE DISCUSSION

The aim of this work was to propose an efficient analytical design procedure for zero-phase anisotropic 2D filters, belonging to the same class: elliptically-shaped filters, with circular (isotropic) filters as a particular case. As a comparative reference to existing works, other analytical techniques for designing 2D elliptical and circular filters have been previously proposed by the author. Thus, the filters described in [14] and [15] are based on digital prototypes and the frequency mapping leads to low-pass 2D elliptical and circular filters with complex coefficients, more difficult to implement. The filters proposed in [16] are based on zero-phase prototypes and are somewhat related to the ones proposed here; however, the frequency transformation used relies on Euler approximation and bilinear transform, which are known to introduce shape distortions. To the best of author's knowledge, BP Gaussian elliptical filters have not been approached previously.

A rigorous comparison in terms of performance with state-of-the-art oriented filters of this shape is quite difficult to be made, due to the large variety of filters and methods found in the literature. Design approaches like [4] (using McClellan transform for magnitude approximation), [5] (set of filters using multiscale techniques) or [6] (obtaining near-elliptical symmetry by adjusting parameters), as well as the circular filters in [10] and [11] are very different from the one proposed here and lead to filters with other purposes and characteristics, so they are difficult to compare with our proposed method.

The Gaussian filter was chosen as prototype for an elliptically-shaped 2D filter due to its advantages. It can be efficiently approximated as a ratio of even polynomials (in our case of order 4, given by (2)) and can be scaled on the frequency axis to adjust its selectivity, according to (3), as shown in Fig. 1a. For very selective filters, the Gaussian shape is probably the ideal one. Its frequency response is zero-phase; the frequency components will not be phase-shifted, so image distortions will not occur. The resulted filters have an accurate shape, with negligible distortions, even for large bandwidth, close to frequency plane margins.

A major advantage of the proposed directional filters is that they preserve the same order regardless of directional selectivity, since they simply result applying the same frequency mapping (25) to basically the same prototype, which is narrower or wider, as specified by the selectivity scaling parameter *p*. Therefore, it should have the same architectural complexity, which is beneficial from implementation point of view.

The proposed design method is entirely analytical, without using any global optimization techniques; the directional filters designed analytically have also the advantage of being adjustable or tunable, since their matrices determined by (32), (33), (38), (39) depend explicitly on the specified parameters (semi-axes E and F, orientation angle φ, peak frequency ω_0 and scaling parameter *p*). For any given parameter values, the particular filter matrices result directly, following the steps of the design algorithm in section 3.4. Therefore an advantage of the method is its versatility; the design need not be resumed each time again from the start for various specifications. Moreover, the overall 2D filter matrices result directly as convolutions of smaller-size matrices, which may be a useful feature in implementation. This implies that a given image filtering may be implemented sequentially, in several successive steps, being computationally efficient.

6. CONCLUSIONS

The proposed analytical design technique is simple and efficient. In order to derive 2D elliptical or circular filters, a specific frequency transformation was determined, using Chebyshev-Padé approximation. This mapping is applied to the factored, LP or BP Gaussian prototype, thus leading directly to the frequency response of the desired 2D filter, which also results factored, thus simplifying its implementation. Due to the accuracy of used approximations, the frequency response results with a very precise, correct elliptical shape, without any distortions even near the frequency plane limits. The main advantage of the method is that the resulted filter is parametric, in the sense that the filter matrices contain explicitly the imposed specifications (orientation, shape and selectivity); therefore, the filter is adjustable and once given the specifications, the filter matrices are already determined; moreover, they can be written as convolutions of small size matrices. Another benefit of the method is that, due to prototype scalability, all designed 2D filters result of the same order, regardless of their specified selectivity; this feature is also very useful from implementation viewpoint.

REFERENCES

1. W. LU, A. ANTONIOU, *Two-dimensional digital filters*, CRC Press, 1992.
2. N. NAGAMUTHU, M.N.S. SWAMY, *Analytical methods for the design of 2D circularly symmetric digital filters using McClellan transformation*, IEEE ISCAS 1989, Portland, US, May 8-11, 1989, Vol. 2, pp. 1095−1098.
3. C.-K. CHEN, J.-H. LEE, *McClellan transform based design techniques for two-dimensional linear-phase FIR filters*, IEEE Trans. on Circuits and Systems I, **41**, *8*, pp. 505−517, 1994.
4. D. NGUYEN, M. SWAMY, *Approximation design of 2-D digital filters with elliptical magnitude response of arbitrary orientation*, IEEE Trans. on Circuits and Systems, **33**, *6*, pp. 97−603, 1986.
5. S.A. JACKSON, N. AHUJA, *Elliptical Gaussian filters*, Proc. 13th Int. Conf. on Pattern Recognition, Vienna, August 25-29, 1996.
6. C.L. KEERTHI, V. RAMACHANDRAN, *Study of elliptical symmetry in 2D IIR Butterworth digital filters*, Proc. of IEEE 47th Midwest Symposium Circuits & Systems, MWSCAS 2004, July 25-28, 2004, Vol. 2, pp. 77−80.
7. K.N. CHAUDHURY, A. MUNOZ-BARRUTIA, M. UNSER, *Fast space-variant elliptical filtering using box splines*, IEEE Trans. on Image Processing, **19**, *9*, pp. 2290–2306, 2010.
8. J.M. ABDUL-JABBAR, Z.N. ABDULKADER, *Iris recognition using 2-D elliptical-support wavelet filter bank*, 3rd Int. Conf. Image Processing Theory, Tools and Applications (IPTA), Istanbul, October 15-18, 2012.
9. Y. ZHANG, *Fingerprint image enhancement based on elliptical shape Gabor filter*, 6th IEEE Int. Conf. Intell. Syst., Sofia, 2012.
10. C. GUILLEMOT, R. ANSARI, *Two-dimensional filters with wideband circularly symmetric frequency response*, IEEE Trans. on Circuits and Systems II, **41**, *10*, pp. 703–707, 1994.
11. M.T. HANNA, *Design of circularly symmetric two-dimensional linear-phase low-pass FIR filters using closed-form expressions*, IEEE Trans. on Circuits and Systems II, **43**, *7*, pp. 537−540, 1996.
12. V. LAKSHMANAN, *A separable filter for directional smoothing*, IEEE Geoscience and Remote Sensing Letters, **1**, pp. 192−195, 2004.
13. S.Y.M. LAM, B.E. SHI, *Recursive anisotropic 2-D Gaussian filtering based on a triple-axis decomposition*, IEEE Trans. Image Processing, **16**, *7*, pp. 1925–1930, 2007.
14. R. MATEI, *Analytical design of elliptically-shaped 2D recursive filters*, IEEE 61st Intl. Midwest Symp. on Circuits and Systems MWSCAS 2018, Windsor, Ontario, Canada, August 5-8, 2018, pp. 964−967.
15. R. MATEI, *Closed-form design of 2D filters with elliptical and circular frequency response*, Proceedings of the 24th European Conference on Circuit Theory and Design (ECCTD), Sofia, Bulgaria, September 7-10, 2020.
16. R. MATEI, P. UNGUREANU, *Image processing using elliptically-shaped filters*, Proceedings of IEEE International Symposium on Signals, Circuits and Systems (ISSCS 2009), Iasi, Romania, July 9-10, 2009, Vol. 2, pp. 337−340.
17. R. MATEI, *Analytical design methods for directional Gaussian 2D FIR filters*, Multidimensional Systems and Signal Processing, **29**, *4*, pp. 185−211, 2018.
18. R. MATEI, *Analytic design of directional and square-shaped 2D IIR filters based on digital prototypes*, Multidimensional Systems and Signal Processing, **30**, *4*, pp. 2021−2043, 2019.
19. R. MATEI, *A class of directional zero-phase 2D filters designed using analytical approach*, IEEE Transactions on Circuits and Systems I: Regular Papers, **69**, *4*, pp.1629−1640, 2022, doi: 10.1109/TCSI.2021.3139141.
20. https://osf.io/de3vm/

Received August 8, 2021